Techno-economic analysis using different types of hybrid energy generation for desert safari camps in UAE

Ali Saleh AZIZ*
Department of Medical Instrumentation Engineering Techniques, Al-Hussain University College, Karbala, Iraq

Abstract: Remote areas in UAE are still fully powered by diesel generators. The rapid rise in the prices of petroleum products and environmental concerns have led to demand for hybrid renewable energy generators. Advances in renewable energy technologies impart further impetus to techno-economic power production. Protecting the landscape and demography of the desert by optimizing the power supply cost via an efficient hybrid power system is the key issue. Simulation results on the cross utilization of a photovoltaic/wind/battery/fuel-cell hybrid-energy source to power the off-grid living space are presented. Simultaneous exploitation of different renewable energy sources to power off-grid applications together with battery and hydrogen energy storage options is demonstrated. HOMER software from the National Renewable Energy Laboratory (NREL) is used to perform detailed techno-economic analyses. It simulates all possible system configurations that fulfil the suggested load for the selected sites under given conditions of renewable resources.

Key words: Hybrid, wind speed, solar radiation, HOMER software, total net present cost (NPC)

1. Introduction

Desert safari camps in the United Arab Emirates (UAE) are attractive to tourists and residents for activities such as sand skiing, camel riding, barbeques, and dancing. The characteristic long hours of sunshine throughout the year and beautiful desert landscape are fascinating. Camps are built deep in the desert and isolated from any civilization to provide a real sense of the culture. Consequently, use of diesel generators is inevitable because they are remotely located from electric grid lines. Furthermore, the generators' operational noise and associated vibrations force them to be installed 30–40 m away from the camp. The generator capacities range from tens to hundreds of kVA depending on the safari size. Apart from emissions, the diesel leakage from generators is found to pollute the natural underground water resources. In this view, use of new energy resources in an inexhaustible clean and silent fashion is the only alternative to fossil fuels. Keshtkaran et al. [1] introduced a method to optimize the size of a hybrid system, where different components including fuel cell, photovoltaic (PV), and diesel generator are used for supplying power in a desert safari camp in UAE. They considered the running cost of hydrogen, PV cleaning, and diesel. Their prime objective was to reduce the use of diesel generators and to minimize the emission of pollutants and overcome other shortcomings. The PV/diesel/battery is found to be the best optimal power system for the desert safari camp, whereas the stand alone fuel cell is the most expensive system. Despite many efforts, the development of efficient renewable energy systems that may lead to zero carbon scenarios and minimal fuel injection in the desert camp is far from being realized.

---

*Correspondence: iraq_1991@yahoo.com

Sufficient research on the application and role of renewable technology with zero emissions has been done. Nandi et al. [2] performed a techno-economic analysis and optimization of an autonomous hybrid wind/PV power system considering the total system cost and the unit cost of the produced electricity. They demonstrated that an optimum combination of the hybrid wind/PV power system achieved higher performance than either of the single structures for the same cost of every battery storage capacity.

Another study [3] presented a case study of a wind/PV hybrid system with a peak load of 1.15kW installed capacity developed in hilly terrain in India. This study showed that the most economical system consists of a 2-kWp PV system with 1 string of ten 12-V batteries. The results indicated that PV and wind turbine can be utilized economically using solar/wind hybrid energy systems for decentralized applications.

PV and wind turbine are favourable technologies for supplying load in remote and rural areas. However, renewable energy systems based on intermittent sources exhibit strong short-term and seasonal variations in their energy outputs. Hybrid wind/PV energy systems efficiently combine complementary characteristics of wind and solar sources to improve its reliability and reduce the cost [2].

The feasibility of techno-economic and optimal design of an autonomous hybrid wind/PV/fuel cell/battery power system that has zero emissions via mathematical modelling and simulation to power the safari camp of Al-Ain city is discussed in this paper. The effects of ambient temperatures, load variations, and PV slopes and azimuth are considered.

2. Materials and methods
2.1. Description of HOMER software

The HOMER computer software developed by National Renewable Energy Laboratory (NREL) of the United States is used in our simulation. It is used to identify the operational characteristics of different renewable energy sources by considering the technical and economic features of system. Moreover, sensitivity analysis can be performed to determine the impact of changing some variable parameters such as the fuel cost on the cost of energy [4].

2.2. Cost optimization

Firstly, the technical feasibility of the system capability in satisfying the load demand is assessed by HOMER. Then it calculates the total net present cost (NPC) of the system (the total cost of the project). Net present cost, which includes capital cost, replacement costs, operation and maintenance costs, fuel costs, and salvage cost, is calculated using [5]

$$NPC = \frac{C_{tot}}{CRF(i,n)}, \tag{1}$$

where C_{tot} is the total cost per year (\$/year), i is the real interest rate (%) per year, and n is the lifetime of the project. The capital recovery factor (CRF) is calculated using [5]

$$CRF(i,n) = \frac{i \times (1+i)^n}{(1+i)^n - 1} \tag{2}$$

The value of NPC is estimated by considering the salvage costs (SC), which are the residual values of the system components at the end of the project lifetime and are calculated by [5]

$$SC = C_{RC} \times \frac{T_{rem}}{T_{com}}, \tag{3}$$

where C_{RC} is the cost of replacement (\$), T_{rem} is the remaining life (year), and T_{com} is the lifetime (year) of the component.

The levelized cost of energy (COE) yields [6]

$$COE = \frac{C_{tot}}{E_{tot}}, \tag{4}$$

where E_{tot} is the annual consumption of the total electricity (kWh/year).

2.3. Case study of a hybrid renewable energy system

2.3.1. Load profile of the camp

A desert safari camp (UAE) as shown in Figure 1 is selected for case study [1]. Figure 2 illustrates the daily electrical load profile of the camp. To give a reliability for the changing in the load for both time-step-to-time-step and day-to-day, random variability of 10% has been considered. The computed values of the scaled annual average of the load, peak load, and load factor are 65 kWh/day, 6.9 kW, and 0.391, respectively.

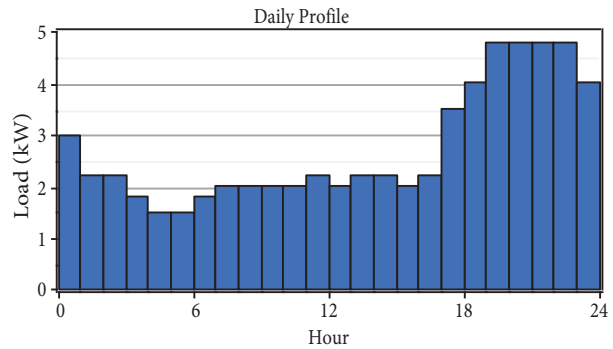**Figure 1.** Desert safari camp in Al-Ain city.

Figure 2. Daily load demand of the camp.

2.3.2. Available renewable energy resources

2.3.2.1. Wind source

Figure 3 depicts the monthly variation of wind speed in Al-Ain indicating diurnal variation. The probability distribution of wind speed is calculated using Weibull's function given by [2]

$$f(v) = \frac{k}{c} \times \left(\frac{v}{c}\right)^{k-1} \times \exp\left[-\left(\frac{v}{c}\right)^{k}\right], \tag{5}$$

where k represents a shape parameter that describes the dispersion of the data, v is the wind speed, and c is the scale parameter having unit of speed (m/s). The average wind speed is related to these parameters through gamma function (Γ) and follows [2]

$$V_{ave} = c \times \Gamma \times \left(\frac{1}{k} + 1\right) \tag{6}$$

The maximum likelihood method is used to fit the measured wind data with this distribution function, which is displayed in Figure 4.
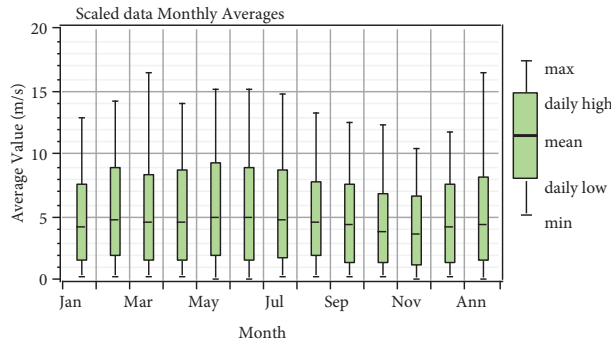
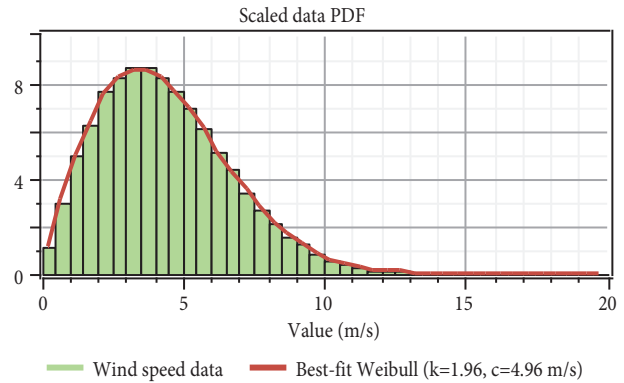**Figure 3.** Monthly average wind speeds in Al-Ain.

Figure 4. Wind speed probability distribution.

2.3.2.2. Solar radiation

In the Al-Ain camp site, the annual average temperature is 27 °C having 60% humidity [7]. Figure 5 depicts the HOMER generated monthly clearness index and daily radiation profile (monthly average) for a year. The data are collected for latitude 22° 11ʹN and longitude 55° 24ʹE [1].
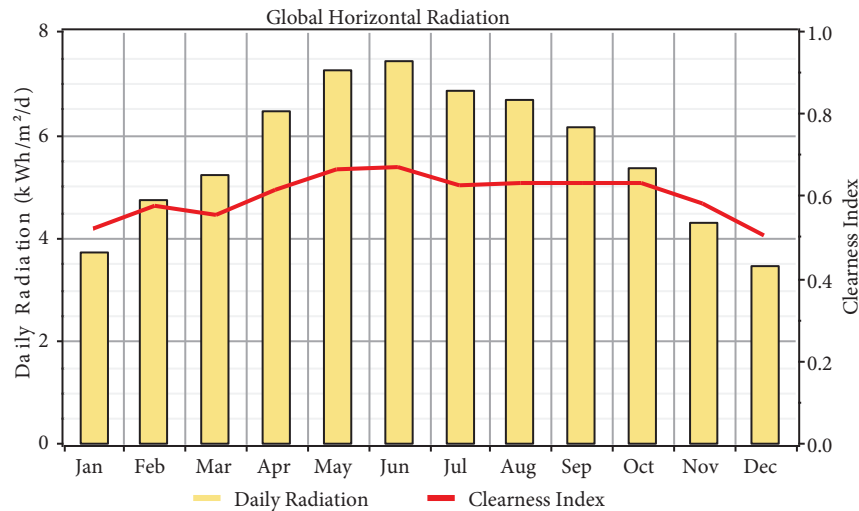

Figure 5. Monthly average solar radiation in Al-Ain camp.

HOMER with PV in terms of rated kW by assuming their outputs linearly proportional to the incident solar radiation. The PV array produces 80% of its rated output if the solar radiation is 0.80 kW/m^2 [8]. The output of the PV array is computed using [4]

$$P_{PV} = Y_{PV} \times f_{PV} \times \left(\frac{\tilde{G}_T}{\tilde{G}_{T,STC}} \right) \times \left[1 + \alpha_P \times (T_C - T_{C,STC}) \right], \tag{7}$$

where Y_{PV} is the rated capacity of the photovoltaic array (kW) signifying its output power under standard test conditions, f_{PV} is the percentage PV de-rating factor, $\tilde{G}_T$ is the solar irradiation episode on the photovoltaic array in the current time step (kW/m^2), $\tilde{G}_{T,STC}$ is the incident irradiation under standard test conditions

(1 kW/m^2), α_P is the temperature coefficient of power (%/$^\circ$C), T_C is the temperature of photovoltaic cell ($^\circ$C) in the current time step, and $T_{C,STC}$ is the temperature of photovoltaic cell at standard test conditions (25 $^\circ$C).

By assuming the temperature coefficient of power is zero, the above equation can be recast as [4]

$$P_{PV} = Y_{PV} \times f_{PV} \times \left(\frac{\tilde{G}_T}{\tilde{G}_{T,STC}} \right) \tag{8}$$

PV input page of HOMER possessing a derating factor is used to compensate for the reduction in the efficiency to achieve more realistic results. Factors such as dust and wiring losses have relatively minute effects on the efficiency compared with the temperature, which is considered to be the predominant one. The default value is 90% for derating factor although a slightly lower value is recommended in very hot climates [8].

2.3.2.3. Influence of ambient temperature

The impacts of ambient temperature on the power of the PV array are considered in this study. That means Eq. (7) is used to calculate output of the PV array. Figure 6 reveals the average monthly air temperature of Al-Ain [9]. The recorded highest temperature is 34 $^\circ$C, in August (summer), and the lowest is 18.8 $^\circ$C, in January (winter). Therefore, the annual average ambient temperature is $\sim$27 $^\circ$C.
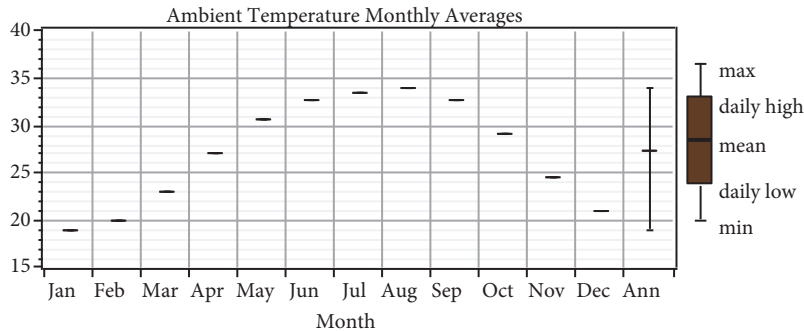

**Figure 6.** The monthly averaged air temperature in Al-Ain, UAE.

2.4. System components

2.4.1. Wind turbine

A turbine that converts the kinetic energy of the wind into DC or AC electricity through the output power dependent wind speed profile at hub height is used in HOMER [10]. The power curve of the SW whisper 500 wind turbine with a capacity of 2.5 kW DC employed in the present study is illustrated in Figure 7. The technical information of the wind turbine is listed in Table 1 [11].

2.4.2. PV module

The photovoltaic module in HOMER generates DC electric current in direct proportion to the global solar radiation irrespective of the exposed temperature and voltage [2]. The technical data of the PV module are summarized in Table 2 [4].
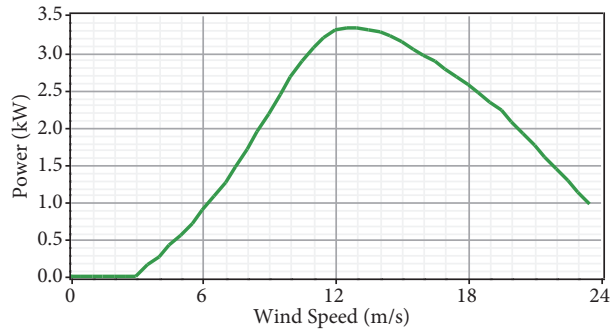
Figure 7. Wind power curve of SW whisper 500 wind turbine.

Table 1. Technical data of SW whisper 500 wind turbine.

Parameters	Value
Diameter of rotor	4.5 m
Rated power	3 kW DC
Cost of capital	$9500
Cost of replacement	$9000
Cost of operating and maintenance	$250/year
Lifetime	15 years
Quantities	0, 2, 3, 4, 6, 7, 8, 9 to 18, 20, 24, 26, 28,

Table 2. Technical data of PV module.

Parameters	Value
Rated capacity	1 kW
Derating factor	90%
Temperature of nominal operating cell	47 °C
Temperature coefficient	$-0.5\%/°C$
Efficiency under standard test condition	13%
Ground reflectance	20%
Cost of capital	$5000/kW
Cost of replacement	$2500/kW
Cost of operating and maintenance	$3/kW/year
Lifetime	25 years
Sizes considered	0, 6, 8, 9 to 18, 20, 24, 26, 28, 30 to 36 (kW)

2.4.3. Storage battery

Energy storage is required to supply the load when the total output power of the photovoltaic and wind turbine is more than the power required by the load. This is because of the stochastic nature of renewable energy resources. The Hoppecke 12 Opzs 1500 is chosen as the storage battery in this paper. Each string consists of two units of batteries. The technical data of the battery are furnished in Table 3 [11].

2.4.4. Electrolyzer

The electrolyzer works through simple water electrolysis, where the DC current source is connected to two electrodes that are placed in the water. Water is decomposed into hydrogen and oxygen and the hydrogen appears at the anode [12]. The technical data of the battery are summarized in Table 4 [13].

Table 3. Technical data of Hoppecke 12 Opzs 1500 battery.

Parameters	Value
Nominal voltage	2 V
Nominal capacity	1500 Ah (3 kWh)
Cost of capital	$508
Cost of replacement	$475
Cost of operating and maintenance	$18/year
Minimum lifetime	4 years
Quantities	20 to 55

Table 4. Technical data of electrolyzer.

Parameters	Value
Rated capacity	1 kW
Efficiency	75%
Cost of capital	$2000/kW
Cost of replacement	$1500/kW
Cost of operating and maintenance	$ 20/kW/year
Lifetime	15 years
Quantities	0, 3, 5, 6, 8, 10 to 16, 18, 20, 22–24, 26, 28, 30, 31 (kW)

2.4.5. Hydrogen tank

The daily and seasonal variance between energy source availability and energy needed is overcome by using the hydrogen storage as an energy carrier. For most applications, a pressurized tank is the most cost-effective means of hydrogen storage [14]. The technical data of the hydrogen tank module are summarized in Table 5 [15].

Table 5. Technical data of hydrogen tank.

Parameters	Value
Rated capacity	1 kg
Cost of capital	$1300/kg
Cost of replacement	$ 1200/kg
Cost of operating and maintenance	$15/kg per year
Lifetime	25 years
Quantities	0,7, 9 to 18, 20, 30, 35, 40, 45, 50, 55, 57 to 70 (kg)

2.4.6. Fuel cell

Production of electricity through the reaction of hydrogen and oxygen in the presence of an electrolyte is achieved using an electrochemical device called a fuel cell. It differs from the battery in that it is does not need to be recharged. It can continuously generate electricity as long as these inputs are supplied [15]. The technical data of the fuel cell module are listed in Table 6 [15].

2.4.7. Inverter

An inverter is used to convert the DC power into conventional AC power with an ability to provide backup power during a power outage [16]. The technical data of the inverter module are supplied in Table 7 [15].

Table 6. Technical data of the fuel cell.

Parameters	Value
Rated capacity	1 kW
Cost of capital	$3000/kW
Cost of replacement	$1500/kW
Cost of operating and maintenance	$0.02/kW per h
Lifetime	5 years
Quantities	0, 2, 3, 4, 5 to 10 (kW)

Table 7. Technical data of the inverter.

Parameters	Value
Rated capacity	1 kW
Efficiency	90%
Cost of capital	$800/kW
Cost of replacement	$750/kW
Cost of operating and maintenance	$0/kW per h
Lifetime	15 years
Quantities	0, 2, 3, 4, 5 to 10 (kW)

2.5. Control strategy

Figure 8 shows the control strategy of the hybrid system. The maximum power point tracker (MPPT) is the control unit of the PV array in order to extract the maximum value of energy despite the variation in weather conditions. Both PV and wind turbine work to feed the load demands. When the output power of these energy sources (depending on the wind speed and the solar radiation variations) is abundant, the generated energy feeds the batteries to be fully charged to power after satisfying the load demand. Once the batteries are fully charged, the energy produced by these systems is supplied to the electrolyzer and the resulting hydrogen is stored in the appropriate tanks. When the energy of the photovoltaic and wind turbine is not enough to supply the load, the energy is supplied by the batteries only or shared between the PV and wind turbine and the batteries. Over an extended time span the batteries get discharged and the fuel cell starts supplying the load with energy stored in the hydrogen tanks automatically.

3. Simulation results and discussion

3.1. Optimization

A system is said to feasible if it meets the required load. The program eliminates all infeasible systems and computes the net present cost (NPC). An optimized hybrid system is achieved via the analyses of different hybrid options. The comparison of all feasible systems is listed in Figure 9.

It is clear that the hybrid wind/PV/battery system with 10 kW of PV arrays, 3 wind turbines of 3 kW, 70 strings of batteries each of 3 kWh, and 8 kW sized power converters is the best optimal power generator for the desert safari camp. The proposed optimal hybrid system is found to have an initial cost of $120,460, an annual operating cost of $3273/year, a total net present cost (NPC) of $162,302, and a levelized cost of energy (COE) of 0.535 $/kWh.

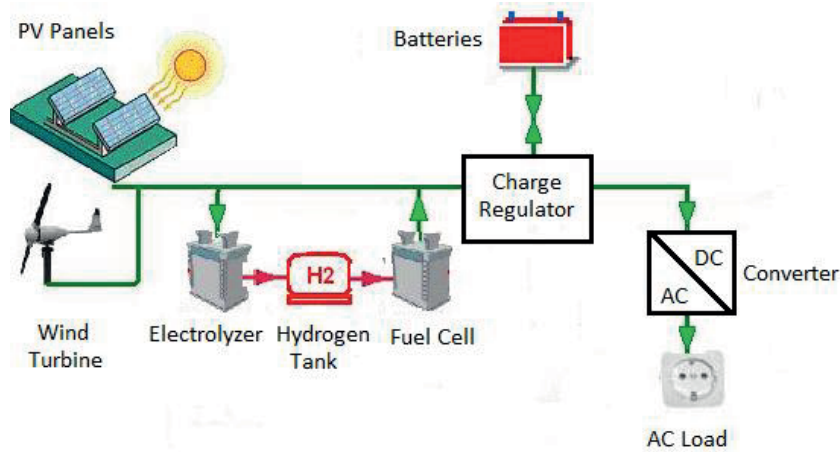The monthly average electric production from the optimized hybrid wind/PV/battery power system is

Figure 8. Control strategy of the hybrid system.

	PV (kW)	W500	FC (kW)	H1500	Conv. (kW)	Elec. (kW)	H2 Tank (kg)	Initial Capital	Operating Cost ($/yr)	Total NPC	COE ($/kWh)	Ren. Frac.	FC (hrs)	Batt. Lf. (yr)
	10	3		70	8			$ 120,460	3,273	$ 162,302	0.535	1.00		20.0
	16			108	8			$ 141,264	2,701	$ 175,797	0.579	1.00		20.0
	10	3	3	70	8	3		$ 135,460	3,319	$ 177,893	0.586	1.00	0	20.0
	16		3	108	8	3		$ 156,264	2,748	$ 191,388	0.631	1.00	0	20.0
		8	8	60	8	5	15	$ 166,380	5,719	$ 239,493	0.789	1.00	263	20.0
	10	7	7		8	13	16	$ 190,700	6,299	$ 271,227	0.893	1.00	4,134	
		12		100	8			$ 171,200	8,338	$ 277,785	0.915	1.00		20.0
		11	8		8	13	68	$ 249,300	9,726	$ 373,632	1.231	1.00	4,892	
	34		8		8	30	68	$ 348,800	5,460	$ 418,595	1.379	1.00	4,884	

Figure 9. Ranking of optimization results according to the NPC of each system type.

displayed in Figure 10. It is evident that the PV array serving as the base load is mostly operational in comparison to the wind turbine. Simultaneously, the monthly average electric production matches the monthly load. The electric generation in May and June is the maximum because of the highest demand during this period.
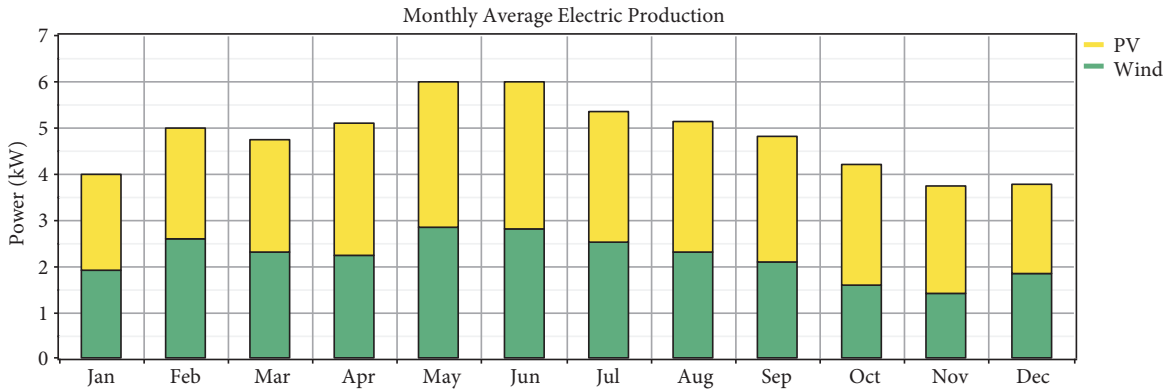

Figure 10. Monthly average electric production from the optimized hybrid wind/PV/battery power system.

The total annual electricity production from the optimized system is observed to be 42,200 kWh/year, of which 23,044 kWh/year (55%) comes from solar radiation and 19,156 kWh/year (45%) of the electricity is drawn from the wind source. The optimized system produces an excess or surplus electricity of 14,160 kWh/year (33.6%). Generally, a hybrid system always produces excess electricity, which can be reused by the dump load in the form of a heating or cooling load of the desert camp.

3.2. Economic analysis

Figure 11 presents the cash flow summary of the various components such as the wind turbine, PV modules, batteries, and power converters in the hybrid wind/PV/battery power system. It is evident that the total NPC is maximum for PV modules and minimum for converters. The capital cost of the proposed hybrid power system is estimated to be $120,460 with a replacement cost of $24,137, O & M cost of $26,078, and salvage cost of $–8373. Thus, the total NPC is $162,302.
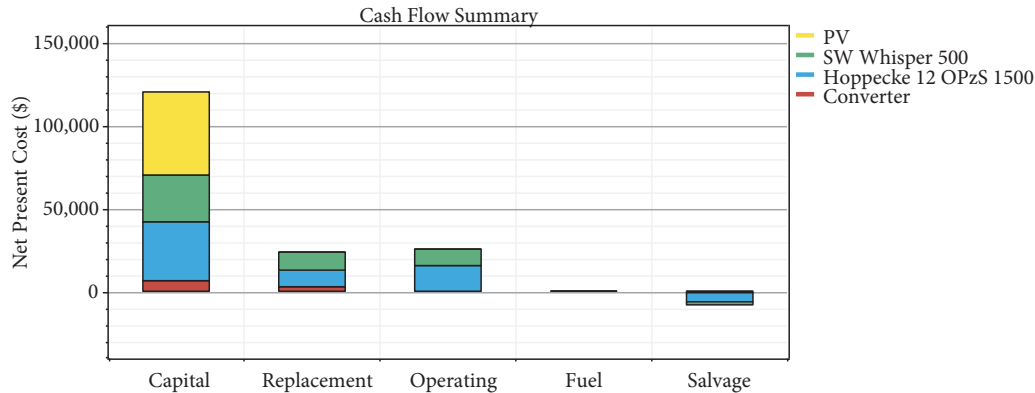

Figure 11. Cash flow summary of the hybrid wind/PV/battery power system.

Keshtkaran et al. [1] demonstrated that the PV/diesel/battery is the best optimal power system for the desert safari camp for the same load with a total NPC of $146,579, which is 10% lower compared to our hybrid PV/wind/battery system. They ignored the effect of temperature on the PV array. However, we considered the effects of temperature variation on the PV array. The increase in temperature causes a reduction in PV output and demands higher PV size. This in turn leads to an increase in the system cost. Conversely, the PV/diesel/battery hybrid system emits pollutants from the diesel generator but our hybrid PV/wind/battery system is far superior, without any emissions.

3.3. PV slope and azimuth analysis

The slope is the angle at which the panels are mounted relative to the horizontal. A slope of $0°$ corresponds to horizontal and $90°$ corresponds to vertical [17]. The azimuth is the direction towards which the PV panels face. Due south is $0°$, due east is $–90°$, due west is $90°$, and due north is $180°$ [18]. Figure 12 shows the slope and azimuth of the PV modules. Here β is the slope and γ is the azimuth positioned to reflect a site somewhere in the northern hemisphere. The position of the sun is described fully using the solar altitude angle (α_s) and azimuth angle (γ_s). Orientation of the slope and azimuth is important to maximize the output of the photovoltaic. Photovoltaics of two axes tracking system installations do not need this consideration since they independently orientate themselves to optimize the output as shown in Figure 13, in which a particular time of

the year is going to be considered, which is 6 January case. Both the slope and azimuth are varying during the day to optimize the output of the PV.
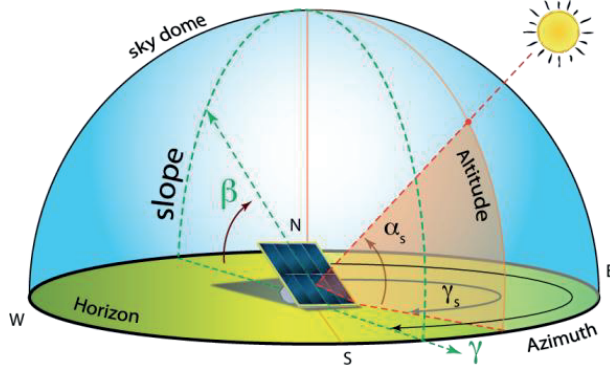

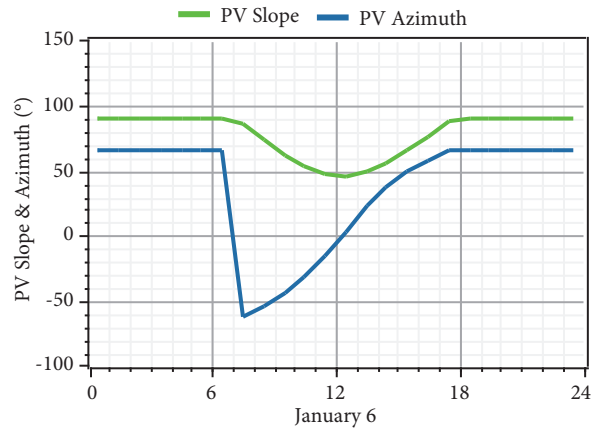**Figure 12.** Slope and azimuth of the PV module.

Figure 13. PV slope and azimuth for 6 January.

3.4. Impact of ambient temperature on the output power of the PV

The temperature of the PV is the temperature of the surface of the PV array. Through the night it is equal to the ambient temperature, while in full sun it can surpass the ambient temperature by 30 $^{\circ}$C or more. The output power of the PV decreases with increasing cell temperature. Figure 14 shows the monthly ambient and cell temperatures. A number of studies have been done to reduce the impact of ambient temperature. Odeh and Behnia [19] presented an efficient method in order to improve the efficiency and limit the rate of thermic degradation of a PV module is by reducing the temperature of its surface. This can be accomplished by cooling the PV array and lowering the heat stored inside the cell of the PV during operation. The experimental results showed that due to the loss of heat by convection between the surface of the PV and water, the output of the system increases by 15% at peak radiation conditions. Zhu et al. [20] presented a general way to radiatively reduce the temperature of a PV cell through sky access, while preserving its solar absorption. They showed that the impact of radiative cooling is substantial, even in the existence of significant convection and conduction and parasitic solar absorption in the cooling layer.
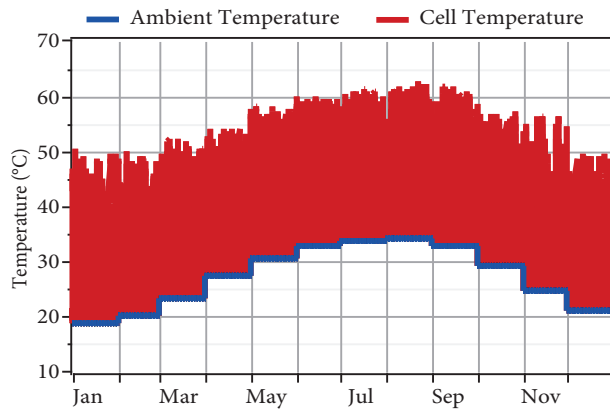

Figure 14. Monthly ambient and cell temperatures.

3.5. Standalone diesel systems

Two diesel generators with capacities of 3 and 5 kW are chosen to meet the power demand of the desert safari camp (6.9 kW). The excess 1.1 kW from the generators caters for the additional loads. The initial and the replacement cost for 6.9 kW generators are considered to be $3450 and $2760, respectively. The appearance of very high operating and maintenance costs ($0.138/h) is related to the remoteness of the area under consideration. Therefore, the 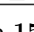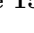omnipresent difficulty in transportation during maintenance indirectly enhances the cost. Each of the installed generators has a lifetime of 15,000 operating hours [21]. Currently, available diesel price in UAE is $0.75 per liter [8]. In this simulation, diesel price is varied to determine its influences on the system because the present global fuel shortage is causing a potential increase in the cost. The impacts of such a high diesel price on the utilization of a standalone diesel system are examined. Eleven values of different diesel prices (0.75, 0.8, 0.85, 0.9, 0.95, 1, 1.05, 1.1, 1.15, 1.2, 1.25 $/L) are considered for sensitivity analysis.

The simulation results reveal that the use of a standalone diesel system corresponding to the diesel price of $0.75/L is the most economical one with total NPC of $108,775 and COE of $0.358/kWh. However, the standalone diesel system using diesel price of $1.25/L gives higher value of the total NPC of $164,759, which is 1% more compared to the use of the hybrid PV/wind/battery system. Figure 15 displays the comparison between diesel generator systems with varying diesel price.

Diesel ($/L)			G1 (kW)	G2 (kW)	Initial Capital	Operating Cost ($/yr)	Total NPC	COE ($/kWh)	Ren. Frac.	Diesel (L)	G1 (hrs)	G2 (hrs)
0.750			3	5	$ 4,000	8,196	$ 108,775	0.358	0.00	8,759	6,955	2,873
0.800			3	5	$ 4,000	8,634	$ 114,374	0.377	0.00	8,759	6,955	2,873
0.850			3	5	$ 4,000	9,072	$ 119,972	0.395	0.00	8,759	6,955	2,873
0.900			3	5	$ 4,000	9,510	$ 125,571	0.413	0.00	8,759	6,955	2,873
0.950			3	5	$ 4,000	9,948	$ 131,169	0.432	0.00	8,759	6,955	2,873
1.000			3	5	$ 4,000	10,386	$ 136,767	0.450	0.00	8,759	6,955	2,873
1.050			3	5	$ 4,000	10,824	$ 142,366	0.469	0.00	8,759	6,955	2,873
1.100			3	5	$ 4,000	11,262	$ 147,964	0.487	0.00	8,759	6,955	2,873
1.150			3	5	$ 4,000	11,700	$ 153,563	0.506	0.00	8,759	6,955	2,873
1.200			3	5	$ 4,000	12,138	$ 159,161	0.524	0.00	8,759	6,955	2,873
1.250			3	5	$ 4,000	12,576	$ 164,759	0.542	0.00	8,759	6,955	2,873

Figure 15. Comparison between diesel generators systems with different diesel prices.

3.6. Harmful gas emissions

Different types of gaseous pollutants such as CO_2, CO, NO_x, SO_2, and unburned hydrocarbon that are emitted during the combustion of fossil fuels are highly damaging for the local environment and adversely affect human life [22]. Table 8 exhibits the emitted pollutants level for the standalone diesel system.

4. Conclusion

This paper proposes different hybrid systems using renewable energy for successfully replacing the stand-alone diesel generators used in desert safari camps in Al-Ain city (UAE). The power sources, which include solar and wind, are exploited. HOMER software developed by the NREL is used to carry out the detailed techno-economic analyses. All possible system configurations that satisfy the demanded load for the selected sites under given conditions of renewable resources are simulated to achieve the optimum design. The effects of ambient temperature on the PV are considered and economic assessment is performed. The optimal hybrid PV/wind/battery power system is achieved with superior efficiency. The hybrid system takes advantage of the

Table 8. Estimate of emitted pollutants from standalone diesel system.

Pollutant	Emissions (kg/year)
Carbon dioxide	23065
Carbon monoxide	56.9
Unburned hydrocarbons	6.31
Particulate matter	4.29
Sulfur dioxide	46.3
Nitrogen oxides	508

Nomenclature	
c	Scale parameter (m/s)
COE	Cost of energy ($/kWh)
C_{RC}	Cost of replacement ($)
CRF	Capital recovery factor
C_{tot}	Total cost per year ($/year)
E_{tot}	Annual consumption of the total electricity (kWh/year).
f_{PV}	Percentage PV de-rating factor
f(v)	Weibull's function
$\tilde{G}_T$	Solar irradiation episode on the photovoltaic array in the current time step (kW/m^2)
$\tilde{G}_{(T,STC)}$	Incident irradiation under standard test conditions (1 kW/m^2)
i	Real interest rate (%) per year
k	Shape parameter
MPPT	Maximum power point trackers
n	Lifetime of the project ($)
NPC	Net present cost ($)
P_{PV}	Output of the PV array (kW)
PV	Photovoltaic
SC	Salvage cost ($)
T_C	Temperature of photovoltaic cell (°C) in the current time step
T_{com}	Lifetime of the component (year)
$T_{(C,STC)}$	Temperature of photovoltaic cell at standard test conditions (25 °C)
T_{rem}	Remaining life (year)
v	Wind speed (m/s)
V_{ave}	Average wind speed (m/s)
Y_{PV}	Rated capacity of the photovoltaic array (kW)
α_P	Temperature coefficient of power (%/°C)
α_s	Solar altitude angle (°)
β	Slope
γ	Azimuth
γ_s	Azimuth angle (°)
Γ	Gamma function

long sunshine hours omnipresent in UAE. The achieved maximum electricity from the PV suggests that it is more feasible than wind turbines at the site. This hybrid system effectively has zero emissions compared to the standalone diesel generator that causes too much air pollution. It is argued that although the use of a standalone diesel system is the cheapest in terms of the current price of diesel, diesel cost is ever increasing, while the price of the PV module and the other system components is expected to fall. Under such circumstances the use of renewable energy sources is demonstrated to be the only future alternative.

References

[1] Keshtkaran E, Fardoun AA, Noura H. Employing hydrogen fuel cell in hybrid energy systems for stand-alone, off-grid remote sites in UAE. In: International Conference on Renewable Energies and Power Quality (ICREPQ'14), 8–10 April 2014; Cordoba, Spain: European Association for the Development of Renewable Energies, Environment and Power Quality (EA4EPQ).

[2] Nandi SK, Ghosh HR. Prospect of wind-PV-battery hybrid power system as an alternative to grid extension in Bangladesh. Energy 2010; 35: 3040-3047.

[3] Rawat R, Chandel SS. Simulation and optimization of solar photovoltaic-wind standalone hybrid system in hilly terrain of India. Int J Renew Energ Res 2013; 3: 696-604.

[4] Li C, Ge X, Zheng Y, Xu C, Ren Y, Song C, Yang C. Techno-economic feasibility study of autonomous hybrid wind/PV/battery power system for a household in Urumqi, China. Energy 2013; 55: 263-272.

[5] Dalton GJ, Lockington DA, Baldock TE. Feasibility analysis of renewable energy supply options for a grid-connected large hotel. Renew Energ 2009; 34: 955-964.

[6] Beccali M, Brunone S, Cellura M, Franzitta V. Energy, economic and environmental analysis on RET-hydrogen systems in residential buildings. Renew Energ 2008; 33: 366-382.

[7] Zoubeidi OM, Fardoun AA, Noura H, Nayar C. Hybrid renewable energy system solution for remote areas in UAE. Global J Technol Optim 2012; 3: 115-121.

[8] Mondal AH, Denich M. Hybrid systems for decentralized power generation in Bangladesh. Energ Sust Dev 2010; 14: 48-55.

[9] Hebah IY. Water demand forecasting in Al-Ain City, United Arab Emirates. MSc, United Arab Emirates University, Abu Dhabi, United Arab Emirates, 2016.

[10] Sunderland K, Woolmington T, Blackledge J, Conlon M. Small wind turbines in turbulent (urban) environments: a consideration of normal and Weibull distributions for power prediction J Wind Eng Ind Aerod 2013; 121: 70-81.

[11] Bataineh A, Alqudah A, Athamneh A. Optimal design of hybrid power generation system to ensure reliable power supply to the health center at Umm Jamal, Mafraq, Jordan. Energ Environ Res 2014; 4: 9-20.

[12] Esmaeili S, Shafiee M. Simulation of dynamic response of small wind-photovoltaic-fuel cell hybrid energy system. Smart Grid Renew Energ 2012; 3: 194-203.

[13] Fahmy FH, Ahmed NM, Farghall HM. Optimization of renewable energy power system for small scale brackish reverse osmosis desalination unit and a tourism motel in Egypt. Smart Grid Renew Energ 2012; 3: 43-50.

[14] Shiroudi A, Taklimi SRH. Demonstration project of the solar hydrogen energy system located on Taleghan-Iran: Technical-economic assessments. In: World Renewable Energy Congress, 8–13 May 2011; Linköping, Sweden: Linköping University Electronic Press; Linköpings Universitet. pp. 1158-1165.

[15] Simmons G. Feasibility of utilizing hydrogen fuel cell systems in hybrid energy systems in stand-alone, off-grid remote northern communities of Canada. MSc, University of Prince Edward Island, Charlottetown, Canada, 2011.

[16] Amjad AM, Salamn Z. A review of soft computing methods for harmonics elimination PWM for inverters in renewable energy conversion systems. Renew Sust Energ Rev 2014; 33: 141-153.

[17] Miloudi L, Acheli D, Chaib A. Solar tracking with photovoltaic panel. Energ Proc 2013; 42: 103-112.

[18] Rowlands IH, Kemery BP, Morrison IB. Optimal solar-PV tilt angle and azimuth: An Ontario (Canada) case-study. Energ Pol 2011; 39: 1397-1409.

[19] Odeh S, Behnia M. Improving photovoltaic module efficiency using water cooling. Heat Transfer Eng 2009; 30: 499-505.

[20] Zhu L, Raman A, Wang KX, Anoma MA, Fan SA. Radiative cooling of solar cells. Optica 2014; 1: 32-38.

[21] Lau KY, Yousof MFM, Arshad SNM, Anwari M, Yatim AHM. Performance analysis of hybrid photovoltaic/diesel energy system under Malaysian conditions. Energy 201; 35: 3245-3255.

[22] Fantidis JG, Bandekas DV, Potolias C, Vordos N. Cost of PV electricity – Case study of Greece. Sol Energ 2013; 91: 120-130.